

## Solutions of Chlorine in Molten Chlorides. 1. Solubility and Diffusivity of Chlorine in NaCl and CsCl Melts

OLE WÆRNES,<sup>a</sup> FRANCESCO PALMISANO<sup>b</sup> and TERJE ØSTVOLD<sup>a</sup>

<sup>a</sup> Institutt for uorganisk kjemi, Norges tekniske høgskole, N-7034 Trondheim-NTH, Norway and

<sup>b</sup> Istituto di Chimica Analitica, Università di Bari, Via Amendola 173, I-70126 Bari, Italy

The reduction of Cl<sub>2</sub> dissolved in molten NaCl, CsCl and NaCl–CsCl eutectic has been investigated by chronopotentiometry. The same value of the diffusion coefficient is obtained by using a plane or a cylindrical working electrode, both made of vitreous carbon.

In the temperature range 510–890 °C the diffusion coefficient of chlorine in alkali chloride melts is in the order of 10<sup>-4</sup> cm<sup>2</sup>s<sup>-1</sup>, and does not seem to be sensitive to the size of the alkali metal cation.

The solubility of chlorine gas in molten NaCl and NaCl–CsCl eutectic has been determined by a manometric technique. This involves keeping the gas volume above the melt constant and to measure the pressure decrease as the gas dissolves in the liquid. The solubility, in the order of 10<sup>-6</sup>–10<sup>-7</sup> mol cm<sup>-3</sup>, increases in the sequence NaCl to CsCl.

A positive enthalpy of dissolution was found for both NaCl and NaCl–CsCl melts.

The main purpose of the present work has been to obtain information on the diffusion coefficients of chlorine dissolved in chloride melts. This is part of a program aimed at an experimental determination of physicochemical parameters that are needed in the model for the back reaction in the magnesium electrolysis.<sup>1,2</sup> The diffusion coefficients together with the solubility of chlorine and magnesium in the melt will be used in a mass-transfer model for the back reaction mechanism.

In recent years there has been an increased interest in molten aluminium chloride–alkali chloride mixtures. One obvious reason for this is the development of a new aluminium process,

which is based on electrolysis of aluminium chloride in alkali and alkaline earth metal chlorides at about 700 °C.

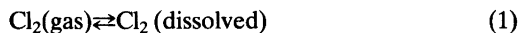
The solubility of chlorine and the kinetics of chlorine reduction in molten chloroaluminates are also important parameters with respect to high energy density batteries.

A paper which deals with solutions of chlorine in chloroaluminate melts will be published later.

Electrochemical methods for the determination of diffusion coefficients of dissolved chlorine in melts require a known chlorine solubility. Due to important improvements in our experimental solubility apparatus it was also of interest to compare our new solubilities with those obtained previously.<sup>3-5</sup>

### PRINCIPLES

*Chlorine solubility measurements.* The following equilibrium is studied:



The equilibrium constant is

$$K = a_{\text{Cl}_2(\text{d})} / a_{\text{Cl}_2(\text{g})} \quad (2)$$

where *a* denotes activity. Assuming that Henry's law is valid for the solute and that Cl<sub>2</sub>(g) is an ideal gas, with standard states of 1 mol cm<sup>-3</sup> for dissolved chlorine and 1 atm for chlorine gas, respectively, the equilibrium constant becomes equal to the Henry's law constant.

$$K = c_{\text{Cl}_2(\text{d})} / P_{\text{Cl}_2(\text{g})} \quad (3)$$

At 1 atm of chlorine pressure the Henry's law constant is equal to the solubility of chlorine. The standard enthalpy of dissolution is given by the equation

$$\Delta H_{\text{d}}^{\circ} = -R \frac{d \ln K_{\text{H}}}{d(1/T)} \quad (4)$$

The Henry's law constant for the dissolution reaction is determined by the relation<sup>3,4</sup>

$$K_{\text{H}} = \Delta P V_{\text{o}} \rho / RT w \Delta P_{\text{eq}} \quad (5)$$

$\Delta P$  is the pressure drop due to dissolution of chlorine,  $V_{\text{o}}$  is the volume of the gas reduced to the thermostated temperature,  $T$ , which normally was 25 °C.<sup>3,4</sup>  $\rho$  is the density of the melt,  $R$  is the universal gas constant (in  $\text{cm}^3 \text{ atm mol}^{-1} \text{ deg}^{-1}$ ),  $w$  is the weight of the salt, and  $\Delta P_{\text{eq}}$  is the change in equilibrium pressure. When initially  $P_{\text{Cl}_2} = 0$ ,  $\Delta P_{\text{eq}}$  equals the final equilibrium pressure ( $P_{\text{eq}}^{\text{u}}$ ).

*Chronopotentiometric measurements.* The fundamental equation for chronopotentiometry (semiinfinite linear diffusion to a plane electrode) is the Sand equation:<sup>6</sup>

$$\tau^{1/2} = \frac{\pi^{1/2} n F A c D^{1/2}}{2I} = \frac{\pi^{1/2} n F c D^{1/2}}{2i} \quad (6)$$

- $\tau$  = transition time
- $n$  = number of electrons in the overall electrochemical reaction
- $F$  = Faraday's constant
- $A$  = electrode area
- $c$  = concentration (solubility of  $\text{Cl}_2$  in the melt)
- $D$  = diffusion coefficient
- $I$  = applied current
- $i$  = current density ( $I/A$ )

It is seen from eqn. (6) that the square root of the transition time is proportional to the concentration of electrolyzed species and inversely proportional to the current. Hence the product  $I\tau^{1/2}$  should be independent of the applied current for given conditions of electrolysis, and the diffusion coefficients may be determined.

Several empirical methods, and also least squares analysis of the chronopotentiogram have been suggested for determination of the transition time from experimental curves.<sup>7-11</sup> In the present study the method of Reinmuth<sup>10</sup> has been used.

Peters and Lingane<sup>12</sup> have derived the follow-

ing equation for chronopotentiometry with cylindrical electrodes

$$I\tau^{1/2} = (\pi^{1/2} n F A c D^{1/2} / 2) \times [1 - (\pi^{1/2} / 4)(D^{1/2} \tau^{1/2} / r) + (1/4)(D^{1/2} \tau^{1/2} / r)^2 - (3\pi^{1/2} / 32)(D^{1/2} \tau^{1/2} / r)^3 + \dots]^{-1} \quad (7)$$

where  $r$  is the working electrode radius, and  $A$  is the area of the cylindrical electrode. In the measurements with cylindrical electrodes, most of the transition times were less than 0.15 s (only very few longer than 0.25 s). Thus the maximum error introduced in  $I\tau^{1/2}$  when the Sand equation is applied, is about 2%. This gives diffusion coefficients which may be up to 4% too large. As eqn. (7) is not strictly valid for the actual electrodes and the approximate correction is relatively small, eqn. (6) has been applied without correction for cylindrical diffusion.

Although the Sand equation is approximately valid when chronopotentiometry is performed with cylindrical electrodes, the accurate determination of the electrode area still remains. In the present study the vitreous carbon rod was immersed in the melt without any kind of shielding. Due to wetting of the rod, a meniscus may rise to a definite height, measured from the melt surface. An increase in the geometrical area,  $A_{\text{geo}}$ , determined from the immersion depth,  $l$ , will thus occur. The total area of the electrode in contact with the melt can thus be divided into two parts

$$A = A_{\text{geo}} + \Delta A = 2\pi r(l + r/2) + \Delta A \quad (8)$$

The area  $\Delta A$  depends on wetting and may also include the influence of the "edge effect" at the end of the rod, and an error in  $A_{\text{geo}}$  due to incorrect determination of the surface level of the melt. This surface level, from which the immersion depth is measured, was determined by slowly lowering the electrode until electrical contact was achieved. A melt drop adhering to the end of the rod during measurements of the surface level will give a too high value for  $l$  and thus for  $A_{\text{geo}}$ . In that case  $\Delta A$  should have a negative value.

From eqns. (6) and (8) at constant concentration it follows that

$$I\tau^{1/2} = kA = kA_{\text{geo}} + k\Delta A \quad (9)$$

$$k = (1/2)\pi^{1/2} F c D^{1/2} \quad (10)$$

A plot of  $I\tau^{1/2}$  versus  $A_{\text{geo}}$  for different immersion depths should therefore yield a straight line. The area  $\Delta A$  may be found from the slope and the intercept of that line. The diffusion coefficient may be determined directly from the slope,  $k$ , according to eqn. (10), or from eqns. (11) and (12) where  $i$  is the current density

$$k = \frac{I\tau^{1/2}}{A_{\text{geo}} + \Delta A} = i\tau^{1/2} \quad (11)$$

$$i\tau^{1/2} = \frac{\pi^{1/2} n F c D^{1/2}}{2} \quad (12)$$

## EXPERIMENTAL

**Chemicals.** The purity of the salts is important for both electrochemical and solubility measurements. Sodium chloride (p.a.) and cesium chloride (p.a. and "Suprapur") from E. Merck AG were employed. Prior to use the salts had to be further purified.

Sodium chloride was dried under vacuum while heating at 400 °C for two hours. The salt was then slowly recrystallized from the melt under nitrogen atmosphere. Only clear crystals were used.

Cesium chloride was purified as follows: The salt was dehydrated with HCl gas up to 400 °C over a period of ten hours, transferred to a quartz glass tube and melted under chlorine atmosphere. The salt was then cooled to about 50 °C below the melting point and evacuated. The chlorine saturation and evacuation were repeated three times and a perfectly clear melt resulted. The salt was then recrystallized from the melt in a quartz glass crucible. The chlorine saturation procedure was important in order to obtain reproducible solubility measurements.

All handling of purified salts were performed in an N<sub>2</sub>-atmosphere glovebox where the water vapour level was constantly monitored and kept below 2 ppm.

Chlorine (>99.8 %) and nitrogen (>99.6 %) from Norsk Hydro a.s., Norway, was used for the electrochemical studies. The gas was passed through concentrated H<sub>2</sub>SO<sub>4</sub> and P<sub>2</sub>O<sub>5</sub> before entering the electrochemical cell. The gas was also passed over graphite heated to 900 °C in order to remove impurities in the gas that could react with the electrodes. Chlorine (>99.6 %) in "lecture bottles" from J. T. Baker Chemicals, Netherlands, was used for purification of salts and for solubility measurements.

HCl gas (>99.8 %), for the drying of salts from Gerling, Holz & Co., FRG and argon

(>99.99 %) from Norsk Hydro a.s., Norway, were used without further purification.

**Electrochemical measurements.** The electrochemical experiments were performed with a potentiostat/galvanostat (Model 551) together with an analog function generator (Model 566) and a multifunction interface (Model 563) from AMEL, Milano, Italy. When operating in galvanostatic mode a pulse generator (made in our workshop) was connected to a mercury-wetted relay in Model 551. This generator was introduced to cut the current at a certain time to prevent metal reduction at the working electrode.

A Tektronix 564 storage oscilloscope (Tektronix, Inc., Beaverton, Oregon) with a Polaroid Land CR-9 camera (Polaroid Corp. Cambridge, Massachusetts) and a Linseis LY 822 X-Y recorder with time base (Linseis GmbH, FRG) were used for data collection and storage.

A Kanthal-wound laboratory tube furnace with three heating zones was used.

The temperature was regulated with a Eurotherm PID regulator and measured with a Pt/Pt10 %Rh thermocouple under the cell close to the outside cell wall. The actual melt temperature was found by a calibration curve correlating melt temperature and temperature outside the cell.

The electrochemical cell was made of a 50 mm diameter quartz glass tube attached to a Pyrex glass cover by a ground conical joint. Electrodes and a quartz glass inlet tube were inserted through S.V.L. screw joints (Sovirel, France) equipped with bored caps and Teflon sealing rings for sliding joints. The upper part of the cell had a side arm for gas outlet. The gas line to the cell was made of Teflon tubing and of the neoprene-like rubber "ISO-Versinic". Connections to the cell and the drying trap were made by "Rotulex" flexible joints and "Torion" valves (Sovirel, France).

A three-electrode system was used. The working electrode was always constructed of a vitreous carbon rod (approx. 3 mm diameter, grade V-25 from Le Carbone-Lorraine, France, or grade GC-30 from Tokai Electrode Mfg. Co. Ltd., Japan). In most of the experiments at temperatures below 550 °C, a plane vitreous carbon working electrode, vacuum sealed into a Pyrex tube was used. After sealing, the end of the Pyrex tube was cut with a diamond cutting wheel. Emery paper was used to polish the plane surface of the electrode. A mirror finish was obtained by lapping with 0.06 micron alumina. Electrical connection to the vitreous carbon rod was made by a thin Pt-wire coiled around the rod before vacuum sealing. The surface area of the electrode

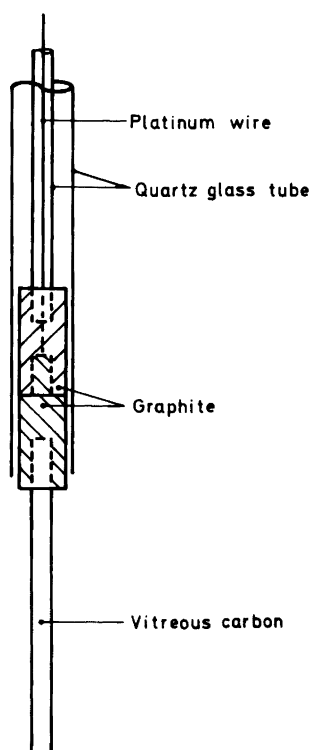


Fig. 1. Cylindrical working electrode.

was determined from the diameter of the vitreous carbon rod as measured by a micrometer screw.

For measurements at temperatures above the softening point of Pyrex glass this electrode could not be used.

A number of materials have been tried without success. Neither boron nitride nor ceramic adhesives gave proper seals with vitreous carbon.

Cylindrical working electrodes with the design shown in Fig. 1 have thus been adopted. The vitreous carbon rod, carefully polished, was press-fitted into a drilled hole at the end of a graphite rod. The electrode was held in place by a 3 mm diameter quartz glass tube through which a platinum wire made contact with the measuring instruments. A Tygon cap fastened the electrode support to a larger quartz glass tube. The working surface area of the electrode was determined from the depth of immersion (accuracy  $\pm 0.01$  mm) as measured by a calliper connected to the outer silica tube.

Both counter and reference electrodes were constructed from spectroscopic grade graphite rods (6 mm diameter, SPK, Union Carbide,

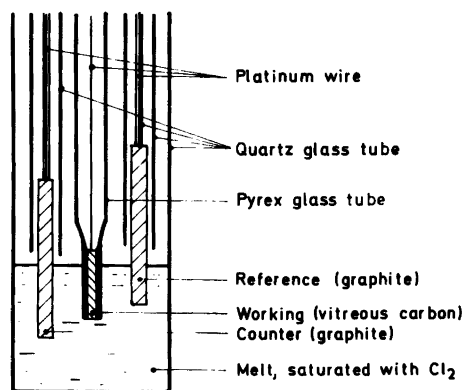


Fig. 2. Electrode assembly used in experiments where a plane working electrode was applied.

Chicago, Illinois). The construction was similar to the cylindrical working electrode previously described (with the exception of the vitreous carbon rod). With  $\text{Cl}_2$  in the melt, the reference electrode may act as a reversible chlorine electrode. The electrode assembly (plane working electrode) is shown schematically in Fig. 2.

Immediately before insertion into the cell the graphite electrodes were heated to a bright orange glow with a torch to remove impurities on the graphite surface. The electrodes were then inserted into the cell which was transferred to a glovebox. The cell was loaded and transferred to the furnace where the salt was melted under nitrogen atmosphere. Before introducing chlorine gas into the cell, cyclic voltammograms in the pure melt were recorded. These showed negligible background current ( $< 50 \mu\text{A cm}^{-2}$ ) within the actual potential range. Following this, the nitrogen was replaced by chlorine by bubbling the gas through the melt for at least three hours. After saturation a slow flow of  $\text{Cl}_2$  was maintained above the melt surface. The same melt was used for electrochemical measurements up to two weeks.

**Solubility measurements.** The method used for measuring chlorine solubility is in principle the same as that used by Andresen,<sup>3</sup> Andresen *et al.*<sup>4,5</sup> and Carpio *et al.*<sup>13</sup> The apparatus which is shown schematically in Fig. 3 has, however, been modified since the previous studies.

Most of the apparatus is made of Pyrex glass, and the essential parts are the manometer (E), the reservoir or calibration bulb (C) and the container for molten salt (A).

The pressure is measured with a manometer (Model 145-01, Precision Pressure Gage, Texas

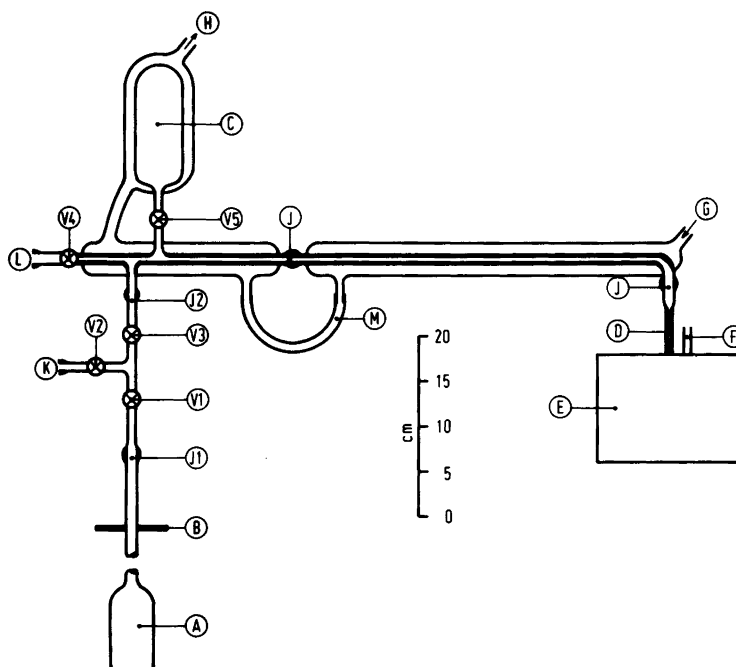


Fig. 3. Apparatus for chlorine solubility measurements. A – quartz glass cell, B – top plate of furnace, C – calibration volume bulb, D – capillary from the Bourdon tube, E – manometer, F – reference port (to vacuum pump), G and H – thermostated water inlet and outlet, respectively, K – vacuum line and gas (argon) inlet, L – chlorine gas inlet, M – plastic tube for thermostated water, v1, v2, v3 – “Interflon” valves, v4, v5 – “Torsion” valves, J – “Rotulex” flexible joints with Viton O-rings.

Instruments Inc., Houston, Texas) with a Bourdon Capsule (Type 800). The Bourdon Capsule assembly consists of a cylindrical case wherein a fused quartz Bourdon tube with attached mirror is mounted. The mirror rotates according to pressure changes within and outside the tube. The pressure gage measures the mirror rotation optically and displays the measurements as a direct pressure readout (in torr) on the digital counter. A data logger (Model 2242B, John Fluke Mfg. Co. Inc., Washington) together with a printer (Model 43, Teletype Corp., Skokie, Illinois) were connected to the external output of the manometer. A calibration curve correlated the output signals (mV) and the digital counter (torr). Pressure changes could also be followed with a strip chart recorder. The Bourdon capsule had no metal parts that could be attacked by chlorine. The solubility apparatus was connected to the pressure port of the Bourdon tube (D). The space surrounding the Bourdon tube was evacuated through the reference port (F) for absolute pressure measurements. A known pressure may also be applied to the reference port,

permitting differential pressure measurements.

A Pyrex to quartz glass graded seal was fused to the pressure port capillary of the Bourdon tube (D). The different parts of the apparatus are connected by “Rotulex” flexible joints with Viton O-rings. The “Torsion” and “Interflon” (G. Springham & Co. Ltd., Essex, England) valves are made with Teflon stems and keys, respectively. The arrangement of joints and valves allowed the cell to be loaded with salt in a glovebox, transferred to the furnace and connected to the apparatus without contact between atmospheric air and salt.

The container for molten salt (A) is made of quartz glass. A “Rotulex” flexible joint was welded to the end of the quartz glass stem by use of a Pyrex to quartz glass graded seal. A water-jacketed, thermostated ( $\pm 0.02$  °C) gas volume serves together with the volume above the melt as the known thermostated gas volume. The reservoir (C) was mainly used for volume calibration. As seen from Fig. 3, part of the gas volume was not thermostated (between B and J2). This part was insulated with styrofoam, and

the change in temperature in this part never exceeded  $\pm 0.5^\circ\text{C}$  during an experiment and a pressure correction could thus be neglected. A variable shunt for the upper zone of the furnace allowed adjustment of the temperature profile. The melt height in the container (A) was about 7 cm. A  $6^\circ\text{C}$  temperature profile over this distance was established in order to impose convection in the melt during dissolution of chlorine.

After the cell had been loaded in the glovebox, valves v1, v2 and v3 (Fig. 3) were closed. The cell was then connected to the apparatus through joint J2, and evacuated. Valve v3 was closed and chlorine added to the rest of the apparatus, which was kept under chlorine pressure between measurements. The salts were then heated under vacuum and allowed to stand overnight for temperature equilibration (argon atmosphere).

By lowering the furnace, salt which had condensed in the neck could be drained back into the cell by melting it with a hand torch.

An experiment started by evacuating the cell ( $P_{\text{eq}}^l=0$ ). Valve v1 was then closed, valve v3 opened and the chlorine pressure adjusted to 900–1000 Torr (valve v5 open). The pressure,  $P_i$ , was recorded on the teleprinter kept in the continuous scan mode. Valve v1 was opened allowing the gas to expand into the cell. The pressure was recorded each fourth second and appeared to be nearly constant within the 10–40 s period after the opening of valve v1. An average value of  $P_o$  for this period is used in the further calculations. The following pressure decrease was recorded on the strip chart recorder. The valve v5 was closed after the determination of  $P_o$ . The equilibrium pressure,  $P_{\text{eq}}^u$ , was assumed to be reached when no further change was observed in pressure (after 1–3 h).  $P_{\text{eq}}^u$  was determined as the average value of ten continuous recorded values on the teleprinter. A volume calibration procedure was performed with  $\text{Cl}_2$  (g) to obtain the unknown volume of gas above the melt,  $V_o$ .<sup>3</sup>

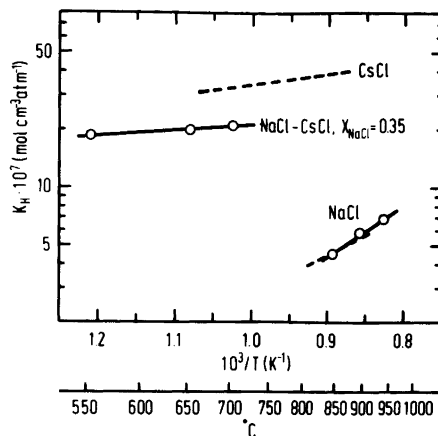


Fig. 4. Semilogarithmic plots of  $K_H$  versus inverse temperature. The dashed lines are results given by Andresen *et al.*<sup>4</sup>

The degassing procedure was as follows: The salt was cooled to about  $20^\circ\text{C}$  above the freezing point, the cell evacuated (valve v3 closed) and the chlorine gas “boiled out” of the melt. The melt was then cooled to  $10^\circ\text{C}$  below the freezing point and then slowly melted again while pumping. Two freeze-melt cycles were necessary to degas the melt. After the degassing procedure, the salt and apparatus were ready for a new solubility measurement.

## RESULTS AND DISCUSSION

**Chlorine solubilities.** The solubilities of chlorine in a fused NaCl–CsCl mixture have been determined in order to calculate the diffusion coefficients of chlorine. For comparison with

Table 1. Solubility of chlorine in molten alkali chlorides.

System	Temperature ( $^\circ\text{C}$ )	$(K_H \pm \text{SD})10^7$ ( $\text{mol cm}^{-3}\text{atm}^{-1}$ )
NaCl	846	$4.54 \pm 0.19$
	892	$5.87 \pm 0.17$
	937	$6.86 \pm 0.50$
NaCl–CsCl	554	$18.5 \pm 0.7$
	652	$19.8 \pm 0.2$
$X_{\text{NaCl}} = 0.35$	701	$21.0 \pm 0.3$

Table 2. Standard enthalpy for the dissolution of Cl<sub>2</sub> in molten alkali chlorides.

System	$\Delta H_d^0$ (kJ mol <sup>-1</sup> )
NaCl	50.7±8.5
NaCl–CsCl (X <sub>NaCl</sub> =0.35)	5.6±1.3
CsCl (Andresen <i>et al.</i> <sup>4</sup> )	11.1±1.9

literature data, solubility measurements in NaCl were also performed.

The Henry's law constants,  $K_H$ , are determined by eqn. (5). The mean values of  $K_H$  with standard deviation are given in Table 1.

According to eqn. (4) a linear relationship exists between the logarithm of the chlorine solubility and the inverse temperature. The enthalpy of dissolution can be determined from the slope of this curve while the intercept with the Y-axis defines the entropy of dissolution. Fig. 4 shows semilogarithmic plots of  $K_H$  (mean values) versus inverse temperature. Straight lines are obtained showing that the solubilities increase with increasing temperature. For comparison selected literature data<sup>3,4</sup> are included (dashed lines).

Linear regression analysis of the experimental data gives the following equations:

$$\text{NaCl:} \\ \log K_H = -3.973 - 2646/T \quad (13)$$

$$\text{NaCl–CsCl (X}_{\text{NaCl}}=0.35\text{):} \\ \log K_H = -5.384 - 290.4/T \quad (14)$$

$$\text{CsCl (Andresen } et al.^4\text{):} \\ \log K_H = -4.882 - 581.3/T \quad (15)$$

The relative standard deviation in  $K_H$  calculated from eqns. (13) and (14) is 8 % and 2.8 %, respectively. From these equations and eqn. (4) the standard enthalpy of dissolution is calculated, and the values are presented in Table 2.

For NaCl  $\Delta H_d^0$  is about 40 % higher than reported by Andresen *et al.*<sup>4</sup> However, it is in close agreement with the value calculated by Andresen *et al.*<sup>4</sup> from data given by Ryabukhin and Bukun.<sup>14</sup>

The values of  $K_H$  in NaCl at low temperatures (801–850 °C) are in good agreement with previous work.<sup>3,4</sup> Due to the 40 % difference in the  $\Delta H_d^0$  value, the deviation in  $K_H$  becomes 12 % at

950 °C. Ryabukhin and Bukun,<sup>14</sup> using the stripping method, report about 40 % lower values of  $K_H$  compared with the present results. The low value for  $\Delta H_d^0$  in NaCl–CsCl eutectic is not surprising as the value in pure CsCl is as low as 11 kJ mol<sup>-1</sup>.<sup>3,4</sup> In binary alkali chloride mixtures it has been observed that  $\Delta H_d^0$  is lower than in the respective pure chlorides.<sup>15–17</sup>

*Diffusion coefficients of chlorine.* Chronopotentiometric measurements have been performed in NaCl, CsCl and NaCl–CsCl melts saturated with chlorine. Representative cathodic chronopotentiometric curves are shown in Fig. 5.

Plots of  $\tau^{1/2}$  versus inverse current were linear at all temperatures. Examples of such plots are shown in Fig. 6. As the curves also pass close to the origin, eqn. (6) is valid, *i.e.* a single diffusion controlled reaction is observed. For experiments using a plane working electrode, the diffusion coefficients of chlorine are thus determined from the mean values of  $i\tau^{1/2}$  at each temperature ( $i$  is the current density). According to eqn. (9) a

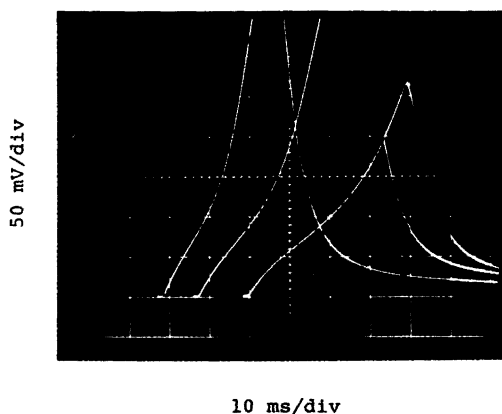


Fig. 5. Chronopotentiometric curves for the reduction of Cl<sub>2</sub> at a cylindrical electrode in molten CsCl at 677 °C. The starting point is shifted to the right for each curve.  $I=35, 30$  and  $25$  mA.

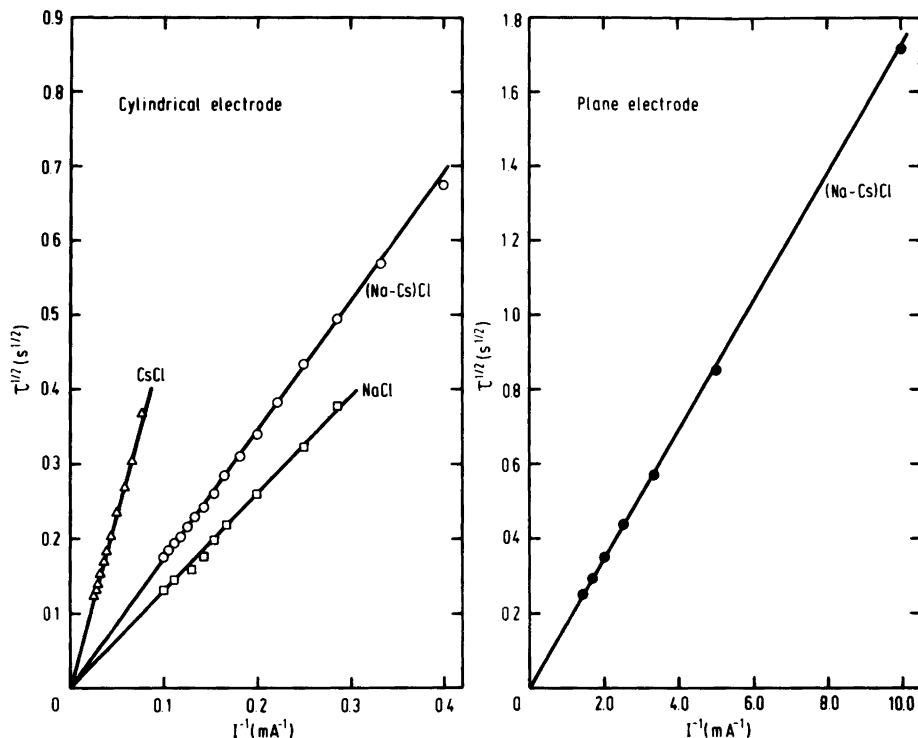


Fig. 6. Test of the Sand equation for the reduction of  $\text{Cl}_2$  at vitreous carbon electrodes.  $\Delta$ : 677 °C,  $A_{\text{geo}}=0.585 \text{ cm}^2$ ,  $\circ$ : 512 °C,  $A_{\text{geo}}=0.523 \text{ cm}^2$ ,  $\square$ : 827 °C,  $A_{\text{geo}}=1.013 \text{ cm}^2$ ,  $\bullet$ : 512 °C,  $A_{\text{geo}}=0.0535 \text{ cm}^2$ .

linear relationship exists between  $I\tau^{1/2}$  and  $A_{\text{geo}}$  when cylindrical working electrodes are used.  $A_{\text{geo}}$  is the surface area determined from the immersion depth of the working electrode. Typical plots are shown in Fig. 7 where the mean value of  $I\tau^{1/2}$  at each immersion depth is plotted versus the corresponding electrode surface area. The chronopotentiometric constant,  $i\tau^{1/2}$ , is given by the slope of this curve [eqn. (11)]. The value of  $i\tau^{1/2}$  at each temperature was determined by linear regression analysis of the data.

Calculated values of  $i\tau^{1/2}$  and values of the diffusion coefficients of chlorine are presented in Table 3. The diffusion coefficients,  $D$ , are determined from the Sand equation [eqn. (6)] where the concentration  $c$  is the chlorine solubility given by eqns. (13) – (15). As the overall electrochemical reaction is



$n$  in eqn. (6) is equal to 2.

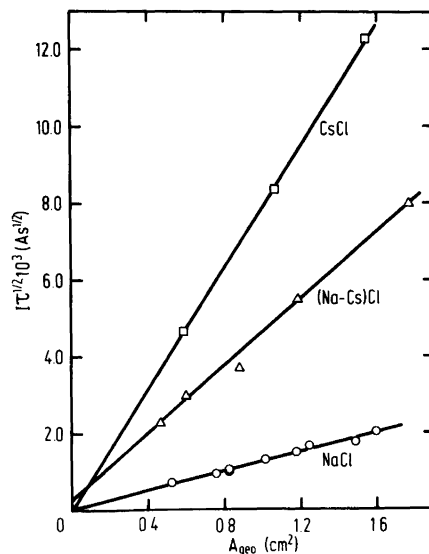


Fig. 7. Mean values of  $I\tau^{1/2}$  versus corresponding cylindrical electrode area,  $A_{\text{geo}}$ .  $\square$ : 677 °C,  $\Delta$ : 647 °C,  $\circ$ : 827 °C



Table 3. Diffusion coefficients of chlorine in molten alkali chlorides determined from chronopotentiometric measurements.

System	Temperature (°C)	Working electrode	Chronopot. constant $(i\tau^{1/2} \pm SD)10^3$ (A cm <sup>-2</sup> s <sup>1/2</sup> )	Number of curves	Diff. coeff. $(D \pm SD)10^5$ (cm <sup>2</sup> s <sup>-1</sup> )
NaCl	827	cylindrical	1.25 ± 0.02	99	30.6 ± 1.0
	887	cylindrical	1.55 ± 0.01	62	26.5 ± 0.3
CsCl	677	cylindrical	8.01 ± 0.04	58	21.3 ± 0.2
	777	cylindrical	9.91 ± 0.07	45	24.9 ± 0.4
	880	cylindrical	11.76 ± 0.09	40	28.0 ± 0.4
NaCl–CsCl $X_{NaCl}=0.35$	512	plane	3.23 ± 0.02	27	11.5 ± 0.1
	512	cylindrical	3.16 ± 0.06	61	11.0 ± 0.4
	647	cylindrical	4.38 ± 0.05	73	16.4 ± 0.4
	797	cylindrical	4.89 ± 0.05	37	16.7 ± 0.3

Both cylindrical and plane working electrodes have been applied for NaCl–CsCl eutectic mixture at 512 °C. The two electrodes gave the same result within the experimental uncertainty.

This confirms that corrections for the cylindricality of the diffusion field may be neglected for certain conditions of electrolysis.

The temperature dependence of the diffusion coefficient is well-described by the Arrhenius-type equation

$$D = D_0 \exp(-E_a^D / RT) \quad (17)$$

where  $D_0$  is a pre-exponential factor, and  $E_a^D$  is the activation energy of the diffusion process. Fig. 8 shows semilogarithmic plots of  $D$  versus inverse temperature. For comparison, selected literature data<sup>7</sup> are included (dashed lines).

Linear regression analysis of the data given in Table 3 gives the following equations:

$$\text{NaCl:} \quad \log D = -4.722 + 1329/T \quad (18)$$

$$\text{CsCl:} \quad \log D = -2.995 - 642/T \quad (19)$$

$$\text{NaCl–CsCl } (X_{NaCl}=0.35): \quad \log D = -3.233 - 553/T \quad (20)$$

The relative standard deviation in  $D$  calculated by eqns. (19) and (20) is 1 and 9 %, respectively. For NaCl the diffusion coefficient is determined at two temperatures only, and no standard deviation is given. The activation energies of diffusion,  $E_a^D$ , are in fair agreement with literature data (Table 4).

For a diffusion-controlled process a positive energy of activation is expected. The observed negative value of  $E_a^D$  for NaCl, calculated from two temperatures only, does not necessarily have a real physical meaning. This will be discussed later.

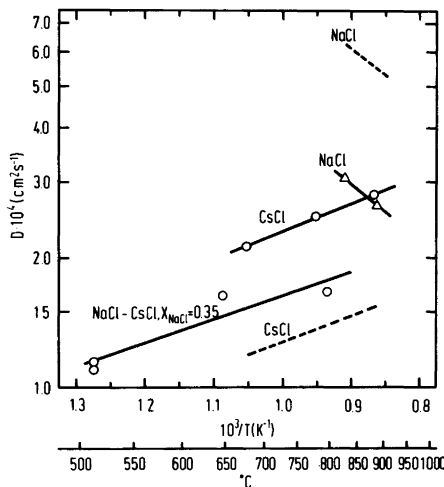


Fig. 8. Semilogarithmic plots of the diffusion coefficient of dissolved Cl<sub>2</sub> as function of inverse temperature. The dashed lines are calculated from data given by Leonova *et al.*<sup>7</sup>

Table 4. Activation energy of diffusion of chlorine in molten alkali chlorides.

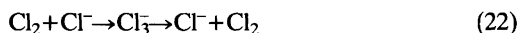
System	$E_a^D$ (kJ mol <sup>-1</sup> )	
	Present work	Leonova <i>et al.</i> <sup>7</sup>
NaCl	-25.4	-22.9
CsCl	12.3±0.4	11.8
NaCl-CsCl ( $X_{\text{NaCl}}=0.35$ )	10.6±2.9	

Diffusion coefficients of Cl<sub>2</sub> in pure NaCl and CsCl do not agree with literature data.<sup>7</sup> This discrepancy may be due to the fact that different solubility data are used in the calculations. When one set of solubility data is used to recalculate the diffusion coefficients of chlorine, improved agreement is obtained.

The relatively high diffusion coefficients of chlorine in molten alkali chlorides have been explained by a chain conduction of the Grotthus' type.<sup>7,15-20</sup> When chlorine is dissolved in the melts the equilibrium



is assumed to be established. The chain conduction is possible if a Cl<sub>3</sub><sup>-</sup> ion transfers a Cl<sub>2</sub> molecule to an adjoining Cl<sup>-</sup> ion which then becomes a Cl<sub>3</sub><sup>-</sup> ion, *i.e.*



The net effect is transport of chlorine molecules. Kowalski and Harrington<sup>21</sup> and Baibakov *et al.*<sup>22</sup> found a rapid exchange between the chlorine gas and <sup>36</sup>Cl<sup>-</sup> isotopes in molten PbCl<sub>2</sub>-KCl and LiCl-NaCl.

Leonova *et al.*<sup>7</sup> and Ukshe *et al.*<sup>20</sup> claim that the diffusion process [eqn. (22)] is assumed to occur most readily in fused salts with small cations (Li<sup>+</sup>, Na<sup>+</sup>) where dense packing allows anion-anion contact. For larger cations, such contact becomes more difficult, *i.e.* lower diffusion coefficients. The negative value of  $E_a^D$  (NaCl) is thus explained as due to increased tendency to form molecular pairs of the type (Na<sup>+</sup>Cl<sup>-</sup>) when the temperature increases. This reduces the possibility for anion-anion contact, *i.e.* the diffusion coefficient of chlorine will decrease with increasing temperature. For salts with large cations (K<sup>+</sup>, Cs<sup>+</sup>), the possibility of

anion-anion contact increases with increasing temperature due to increased vibrational movement and disturbance of the melt structure. A positive value of  $E_a^D$  is therefore found for these melts.

The postulated increased tendency to form molecular pairs of the type (Na<sup>+</sup>Cl<sup>-</sup>) at the actual temperature does not seem to be plausible. No anomaly has been observed in the viscosity of the pure alkali chlorides<sup>23</sup> and approximately the same temperature dependence is found for the viscosities of both NaCl and CsCl. This implies that a positive energy of activation should be expected whatever the cation of the chloride melt and should indicate that the explanation given by Leonova *et al.*<sup>7</sup> to justify the negative value of  $E_a^D$  could be no longer valid. The apparent agreement of the activation energies for the Cl<sub>2</sub> diffusion in NaCl melts found in this work and in Ref. 7 is probably fortuitous and both data could be affected by uncertainties in solubility data and/or electrochemical measurements.

According to Ukshe *et al.*<sup>20</sup> the diffusion coefficients of chlorine in pure alkali chlorides exceed the self-diffusion coefficients of Cl<sup>-</sup> by 1.5-2 orders of magnitude. The values of the self-diffusion coefficients used by Ukshe *et al.*<sup>20</sup> (taken from Bockris and Hooper<sup>24</sup>) are, however, a factor of ten too low. According to Bockris and Hooper,  $D_{\text{Cl}^-}$  in NaCl; increases from  $0.7 \cdot 10^{-4}$  to  $1.1 \cdot 10^{-4}$  cm<sup>2</sup>s<sup>-1</sup> in the temperature range 840-980 °C, while in CsCl  $D_{\text{Cl}^-}$  increases from  $0.4 \cdot 10^{-4}$  to  $0.6 \cdot 10^{-4}$  cm<sup>2</sup>s<sup>-1</sup> (670-790 °C). Grjotheim *et al.*<sup>25</sup> give slightly higher tracer diffusion coefficients of <sup>36</sup>Cl<sup>-</sup> in NaCl;  $9.7 \cdot 10^{-5}$  cm<sup>2</sup>s<sup>-1</sup> and  $1.2 \cdot 10^{-4}$  cm<sup>2</sup>s<sup>-1</sup> at 810 and 912 °C, respectively. In KCl and CaCl<sub>2</sub> at 810 °C Tørklep<sup>26</sup> determined  $D_{\text{Cl}^-}$  to be  $8.9 \cdot 10^{-5}$  cm<sup>2</sup>s<sup>-1</sup> and  $3.8 \cdot 10^{-5}$  cm<sup>2</sup>s<sup>-1</sup>, respectively.

The present results (Fig. 8) indicate that the

diffusion coefficient of  $\text{Cl}_2$  does not vary markedly from an  $\text{NaCl}$  to a  $\text{CsCl}$  melt, and the observed differences are within the experimental uncertainties. The values of  $D$  in these melts are ca. 3 times higher than the self-diffusion coefficients of  $\text{Cl}^-$ .

As slightly higher values of the chlorine diffusion coefficients are measured in alkali chlorides compared with the self-diffusion coefficients of  $\text{Cl}^-$ , the transport of molecular chlorine may occur by a chain conduction mechanism [eqn. (22)]. In any case, the transport does not seem to be sensitive to the size of the alkali cation. This is in agreement with data on the diffusion of iodine in fused alkali iodides where approximately the same value of  $D$  ( $\sim 8 \cdot 10^{-5} \text{ cm}^2 \text{ s}^{-1}$  at  $700^\circ \text{C}$ )<sup>27</sup> was found in both  $\text{NaI}$ ,  $\text{KI}$  and  $\text{CsI}$ .

*Acknowledgements.* Experimental assistance of Bente Faaness and Bjarte Haugsdal is gratefully acknowledged. This work has been supported financially by *Norsk Hydro a.s.* and *Norges Teknisk Naturvitenskapelige Forskningsråd* and also partly by a NATO Research Grant SA. 5-2-05B(808)372(74-77) for a cooperation program between the Institute of Inorganic Chemistry, the Norwegian Institute of Technology and the Institute of Analytical Chemistry, the University of Bari.

## REFERENCES

- Aarebrot, E., Andresen, R. E., Østvold, T. and Øye, H. A. *Light Metals 1977*, 106th AIME Annual Meeting, Atlanta 1977, Vol. 1, p. 491.
- Østvold, T. and Øye, H. A. *Light Metals 1980*, 109th AIME Annual Meeting, Las Vegas 1980, p. 937.
- Andresen, R. E. *Thesis*, Universitetet i Trondheim, Norges tekniske høgskole, Institutt for uorganisk kjemi, Trondheim 1976.
- Andresen, R. E., Østvold, T. and Øye, H. A. In Pemsler, J. P., Braunstein, J., Morris, D. R., Nobe, K. and Richards, N. E., Eds., *Proc. Int. Symp. Molten Salts*, The Electrochem. Soc., Princeton, N.J. 1976, p. 111.
- Andresen, R. E., Paniccia, F., Zambonin, P. G. and Øye, H. A. *Proc. 4th Nordic High Temp. Symp. - NORTEMPS - 75*, Vol. 1, p. 127.
- Delahay, P. *New Instrumental Methods in Electrochemistry*, Interscience, New York 1954.
- Leonova, L. S., Ryabukhin, Yu.M. and Ukshe, E. A. *Sov. Electrochem.* 5 (1969) 190.
- Delahay, P. and Berzins, T. *J. Am. Chem. Soc.* 75 (1953) 2486.
- Delahay, P. and Mamantov, G. *Anal. Chem.* 27 (1955) 478.
- Reinmuth, W. H. *Anal. Chem.* 33 (1961) 485.
- Russel, C. D. and Peterson, J. M. *J. Electroanal. Chem.* 5 (1963) 467.
- Peters, D. G. and Lingane, J. J. *J. Electroanal. Chem.* 2 (1961) 1.
- Carpio, R. A., King, L. A., Ratvik, A. P., Østvold, T. and Øye, H. A. *Light Metals 1981*, 110th AIME Annual Meeting, Chicago 1981, p. 325.
- Ryabukhin, Yu.M. and Bukun, N. G. *Russ. J. Inorg. Chem.* 13 (1968) 597.
- Van Norman, J. D. and Tivers, R. J. In Mamantov, G., Ed., *Symp. on Characterization and Analysis of Molten Salts*, Dekker, New York 1969, p. 509.
- Nekrasov, V. N., Biryukov, V. A., Ivanovskii, L. E. and Mironov, V. S. *Tr. Inst. Elektrokhim. Ural. Nauchn. Tsentr. Akad. Nauk. SSSR* 27 (1978) 57.
- Lenova, L. S., Ryabukhin, Yu.M. and Ukshe, E. A. *Sov. Electrochem.* 5 (1969) 424.
- Lenova, L. S. and Ukshe, E. A. *Sov. Electrochem.* 6 (1970) 871.
- Ukshe, E. A. and Leonova, L. S. *Sov. Electrochem.* 6 (1970) 1376.
- Ukshe, E. A., Leonova, L. S., Yavonova, G. N. and Bukun, N. G. *Sov. Electrochem.* 7 (1971) 373.
- Kowalski, M. and Harrington, G. W. *Inorg. Nucl. Chem. Lett.* 3 (1967) 121.
- Baibakov, D. P., Kukushkin, Yu.N. and Golosov, V. V. *Fiz. Khim. Elektrokhim. Rasplavl. Solei Tverd. Electrolitov.* 1 (1973) 117.
- Brockner, W., Tørklep, K. and Øye, H. A. *J. Chem. Eng. Data* 26 (1981) 250.
- Bockris, J.O'M. and Hooper, G. W. *Discuss. Faraday Soc.* 32 (1961) 218.
- Grjotheim, K., Naterstad, T., Tørklep, K. E. and Øye, H. A. *Electrochim. Acta* 23 (1978) 451.
- Tørklep, K. *Thesis*, Universitetet i Trondheim, Norges tekniske høgskole, Institutt for uorganisk kjemi, Trondheim 1972.
- Ivanovskii, L. E., Nekrasov, V. I., Biryukov, V. A. and Mironov, V. S. *Sov. Electrochem.* 11 (1975) 1285.

Received July 20, 1982.